CERN-BE-2018-001

24 May 2018

Michaela.Schaumann@cern.ch

PcInterlock: Implementation and Operational Experience with the Optics Interlock

M. Schaumann, A. Calia, K. Fuchsberger, J. Wenninger
CERN, CH-1211 Geneva 23

Keywords: LHC, power-converter interlock, phase advance, optics interlock, quadrupole, ATS optics

Summary

In 2016 the luminosity reach of the LHC was increased by reducing the β-function in the main collision points below the design value to $\beta^* = 40\,\text{cm}$. This was possible due to a review of the margins in the collimation hierarchy followed by the implementation of additional measures to ensure the phase advance in defined ranges around the circumference.

The risk of damaging the triplet or the tertiary collimators (TCTs) close to the interaction points in the event of an asynchronous beam dump is minimized by including margins in the collimation hierarchy, which define the β^*-reach. By guaranteeing the phase advance within an acceptable tolerance between the beam dump kicker and the TCTs, those margins can be reduced and operation at lower β^* becomes possible. A new interlock system on the quadrupole magnet currents was put in place to safeguard the stability of the phase advance.

This note describes the technical implementation of this power-converter interlock (PcInterlock) and the strategies used to derive appropriated tolerances to allow sufficient protection without risking false beam dump triggers. The experience with the new PcInterlock settings in 2016-18 are discussed.

Contents

1 Introduction **2**

2 Power-Converter Interlock System **3**
2.1 Basic Principle 3
2.2 Interlocking Strategies 4
2.3 Tolerance Generation for Quadrupoles 5
2.3.1 Configuration Management 5
2.3.2 Computation Procedure 5

3 Quadrupole Current Distribution in Physics **9**

3.1 Main, Matching, Warm and Triplet Quadrupoles 9
3.2 Tune Trim Quadrupoles 10

4 Operational Experience with the new Optics Interlock 11
4.1 Operational Settings in 2016 11
4.2 Operational Settings in 2017 (ATS Optics) 12
4.3 Operational Settings in 2018 (ATS Optics and β^*-levelling) 15
4.4 Tolerance Settings during the Squeeze 15

5 Conclusion and Outlook 16

1 Introduction

Various options for the 2016 operational configuration of the LHC were considered [1, 2]. The main change in the final configuration with respect to the previous year was a reduced β-function of $\beta^* = 40\,\text{cm}$ at the main collision points of ATLAS (IP1) and CMS (IP5) [3]. This value is 15 cm below design [4].

The collimators are ordered in hierarchy such that they protect the aperture everywhere in the ring [5, 6, 7]. Accommodating smaller β^* and still maintaining the protection of the aperture imposes smaller collimator gaps (jaws come closer to the beam). In the unlikely event of an asynchronous beam dump (the dump kicker (MKD) misfires while beam passes) the risk is high to severely damage the triplets or the tertiary collimators (TCTs) in front of the experiments ATLAS and CMS. In such an event, the first part of the beam, passing during the rise of the MKD field, is only partially kicked. Most of these mis-kicked particles are absorbed by the collimator between the MKD and the next quadrupole, the so-called TCDQ, and the secondary collimator TCSP. However, a certain amount of particles is expected to escape. These particles potentially have high oscillation amplitudes and could still damage the TCTs [8, 9].

One way to avoid such damage is to retract the TCT jaws further to gain more space for the beam to pass through and be extracted to the beam dump in the next turn. Alternatively, damage can be avoided by constraining the phase advance between the MKD and the TCT [9]. This principle is illustrated in Fig. 1. The picture shows TCTs at two different phases from the dump kicker: TCT_1 (blue) has a fractional phase difference of about 0° from the MKD, while TCT_2 (red) sits at about 90°. In order to reduce the amount of particles on TCT_2, its jaws have to be retracted further compared to TCT_1. Thus by re-matching the phase advance between the MKD and TCT to be close to 0°, tighter TCT settings are feasible which allows smaller β^*-values. However, it has to be ensured that this phase advance is stable enough to always fulfil the requirements in the event of an asynchronous beam dump.

The phase advance around the circumference (and thus in a given section of the LHC) is defined by the strengths of the quadrupoles. Matching the quadrupole strength to obtain the desired phase advances for the nominal machine configuration, as described in Fig. 1, is intrinsically a safe procedure, since the quadrupole currents involved follow pre-defined functions throughout the LHC cycle. Nevertheless, adjustments during operation (e.g. tune trims) can change the phase advance and could potentially move out the configuration from the safe regime. To prevent such - potentially risky - situations, a new interlocking layer was put in place to constrain the changes in the phase advance during operation (see Chapter 2).

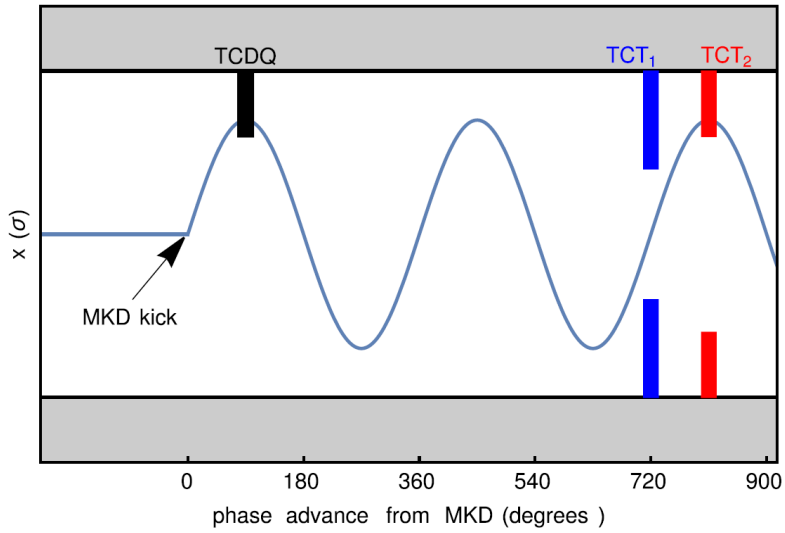

Figure 1: Principle of avoiding damage on the TCTs by constraining the phase advance between MKD and TCT to 0°: If the TCT would be at 90° phase advance, the remaining particles would fully hit the TCTs (case of TCT_2, red). In case of 0° (TCT_1, blue), the beam just passes through the TCTs and no damage occurs. Courtesy of R. Bruce [9]

For the protection during an asynchronous beam dump the phase advances between the MKD and TCTs in IP1 and IP5 are the most critical, particularly during minimum-β^* operation, i.e. after the β^*-squeeze, when the β-function in those interaction points (IPs) is reduced from the large injection ($\beta^* = 11\,\mathrm{m}$) to the small physics (as small as $\beta^* = 0.25\,\mathrm{m}$ in 2018) values. Here the β-functions in the triplets and TCTs are the largest (and with it the beam size), such that the amount of particles potentially impacting on the TCTs is maximized.

2 Power-Converter Interlock System

2.1 Basic Principle

This type of interlock system was introduced for the LHC in 2012 [10]. The Power-Converter (PC) interlock monitors the PC currents to protect against operational- and feedback-failures. Its primary use case, up to now, was the interlock of orbit corrector currents in order to track bump shape amplitudes and variations. To cover the use-case described in this report, it was extended in 2016 to apply an interlock on the optics (phase advance), which is controlled by monitoring the quadrupoles currents. The operational principle of this system is the following:

- A reference current-function is defined for each magnetic circuit (power-converter) to interlock, representing the nominal current evolution for each beam process of the LHC, established at the time of commissioning of the nominal cycle.
- On top of this, each circuit and beam process is assigned a tolerance-function (always positive), specifying how much the current of the given circuit is allowed to vary around the reference.

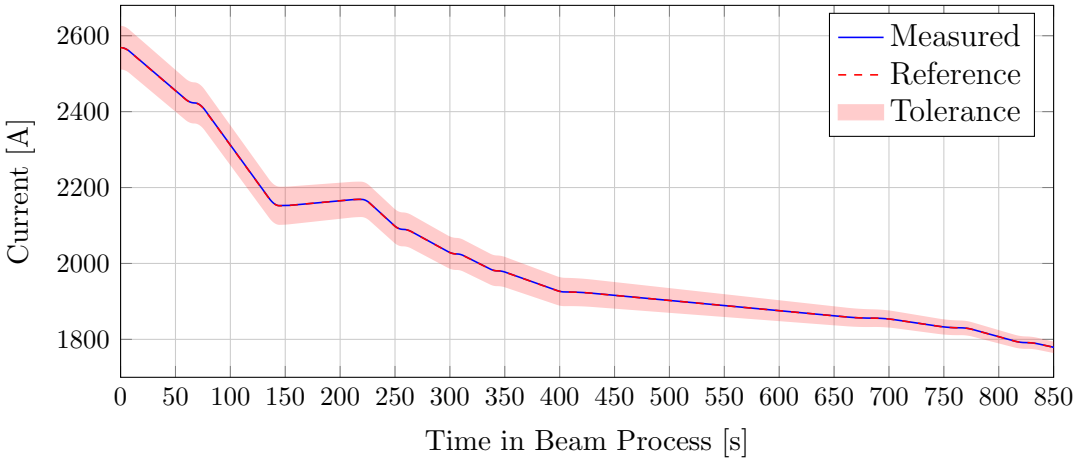

Figure 2: Principle of the PcInterlock. The reference (red dashed) and measured (blue) PC current is shown over the duration of a beam process. The red shade shows the allowed variation tolerance. Once the blue line exceeds the red band, this circuit is considered as interlocking.

- The PcInterlock system takes the measured current of each circuit and checks if the measurement lies within the reference ± tolerance (both corresponding to the actual point in time of the ongoing cycle). In case the measured current is outside the tolerance band, the respective circuit is considered as interlocking.

- Interlock signals are generated based on different strategies, potentially combining interlock signals of several power converters. The beam is dumped as soon as the dump strategy conditions are met.

Figure 2 shows an example of the current evolution of one power-converter during the squeeze as seen by the PcInterlock system. The reference function is shown in red with a shaded red tolerance band. If the measured current (shown in blue) would go out of the tolerance band, the circuit would interlock.

2.2 Interlocking Strategies

As mentioned before, originally the PcInterlock was built to observe all orbit corrector currents with the main purpose to avoid closed orbit bumps. Here the interlock condition is that at least two circuits for one beam and one plane have to be interlocking to trigger a dump, because only in this configuration an unwanted closed orbit bump could build up.

The quadrupole current interlock condition follows a different strategy, since the phase advance between two particular points could be changed by only one arbitrary quadrupole changing its current anywhere on the circumference. Therefore, even if only one individual quadrupole power-converter interlocks a beam dump is triggered. Each interlock output of the PcInterlock (be it orbit correctors or quadrupoles) can have one of the following three states:

- *Ok* → no interlock, current is within limits (or PC is in any other state than *Standby*, *Idle*, *Armed* and *Running*).

- *Warning* → trigger warning, if ≥ 1 PC's current is at 70 % of the interlock limit.

Quadrupole Families	Names	Number of PC
Main Quadrupoles	RQD, RQF	each 1 PC/sector
Main Trim Quadrupoles	RQTD, RQTF	each 1 PC/sector/beam
Triplets	RQX, RTQX1, RTQX2	6 PCs/IP
Matching Quadrupoles	RQ4-RQ10, RQTL9-11, RQT12, RQT13	1 PC each/beam (total count ~ 300)
Warm Quadrupoles	RQ4, RQ5, RQT4, RQT5	1 PC each

Table 1: Quadrupole families in the LHC and the number of responsible power-converters.

- *Interlock* $\rightarrow$ trigger interlock (beam dump). For the quadrupoles, this is the case if ≥ 1 PC's current is at or above 100 % of the interlock limit.

2.3 Tolerance Generation for Quadrupoles

2.3.1 Configuration Management

Tolerances have to be recomputed for every new optics configuration. For this purpose, a simple command line tool, using JMad [11, 12] (an integration of MADX [13] into the Java environment), was developed. To keep the interlock system simple, the interlocking is always done on current-level, since currents are the observable quantities. However, to configure the system it is much more convenient to work on k-level (where k is the magnet strength). Therefore, the tolerances are configured on k-level and stored in the LHC Software Architecture (LSA), from which the PcInterlock takes its settings. LSA internal mechanisms (so-called *makerules*) are used to convert the strength values to currents. LSA is the natural place to perform this transformation, because all required information is already available: e.g. the magnet transfer-functions that describe the relation between the magnet current and the magnetic field, as well as the beam momentum at a given time. For easier configuration, the computation is based on the following simplifications:

- Define magnet families and use the same tolerances in terms of magnet strength, k_{tol}, for groups of magnets with the same purpose. This keeps the number of different tolerance values small for easier maintainability. Currently the defined families correspond to the logical hardware groups in LSA, listed in Table 1.

- All phase-advance changes are taken as absolute values, in order to assume the worst cases scenario (phase advance shifts adding up in the same direction) and avoid sign-convention problems.

2.3.2 Computation Procedure

Deviations from the nominal quadrupole strengths sum up to a total phase error in the machine. The effect on the phase advance by an individual current error in the power-converter is however

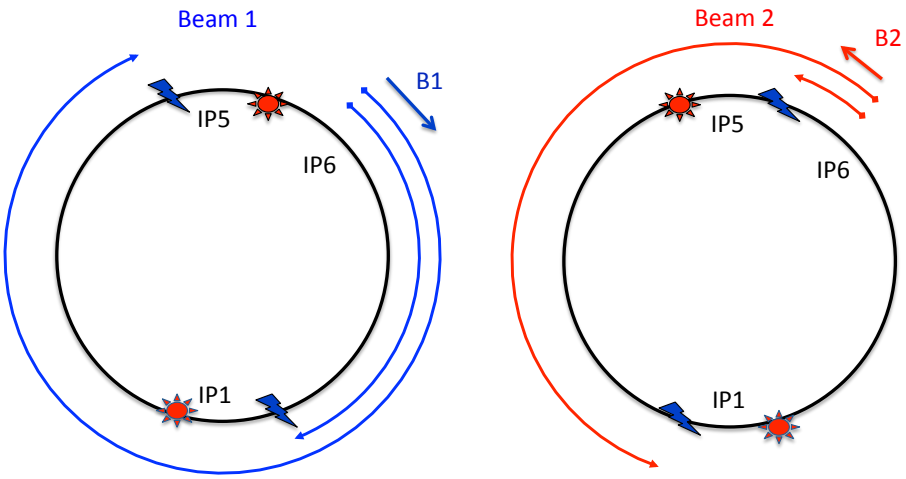

Figure 3: Tolerance generation ranges of the LHC ring.

different for each quadrupole (and thus between the quadrupole families[1]) and depends on the β-function at the quadrupole and thus on its position in the machine. Therefore, individual reference function and tolerances have to be defined for each family.

For the failure case described here, it is enough to consider the four distinct ranges of the LHC circumference as illustrated in Fig. 3: for each beam, the range from the dump kicker (IP6) to the interaction points IP1 and IP5, respectively. The PcInterlock has to ensure the stability of the phase advance in these four segments.

The generation of the individual tolerances is based on MADX simulations of the closed-orbit phase and the maximum allowed phase advance change. Individual computations of the phase advance per PC per segment are performed. All PCs are assigned an individual tolerance according to their family and are interlocked individually.

Allowed Total Phase-Advance Change

The total budget for the allowed phase-advance deviation over any of the segments shown in Fig. 3, $\Delta\mu^{\text{budget}}$, is based on machine protection considerations and computed in [9]. In 2016,

$$\Delta\mu^{\text{budget}}(2016) = 26^\circ \tag{1}$$

was tolerable, while in 2017, with Achromatic Telescopic Squeeze (ATS) optics (see [14] and Section 4.2), only

$$\Delta\mu^{\text{budget}}(2017) = 4^\circ \tag{2}$$

was acceptable. The phase advance was measured with the ATS optics in 2017, revealing a phase shift of 3°. Using this measurement as a reference, the allowed total phase budget could be relaxed to $\Delta\mu^{\text{budget}}_{\text{meas}}(2017) = 7^\circ$.

Magnet Family Tolerances

The calculation described here was revised since Ref. [15], where the family responses and the total phase budget are obtained by calculating the linear sums of all families. This describes

[1] e.g. quadrupoles can be powered individually or in series at very different nominal currents

a situation in which all magnets of all families show a fully correlated error. This is a too pessimistic assumption and not a realistic failure scenario. Most quadrupoles (all except the trim quadrupoles) follow individual, pre-defined functions throughout the accelerator cycle, defined in so-called *beam processes*, and are never modified by other means (e.g. trim knobs). These functions are carefully evaluated with low intensity beam during the commissioning and kept unchanged for the following operational period.

It can thus be assumed that the phase errors between families are uncorrelated. Therefore, the total phase-advance budget from above is distributed over the magnet families with the condition that the quadratic sum of the phase-advance budgets, $\Delta\mu_f^{\text{budget}}$, per family $f \in F$ (F is the set of all defined families), does not exceed $\Delta\mu^{\text{budget}}$:

$$\Delta\mu^{\text{budget}} \geq \sqrt{\sum_{f\in F}(\Delta\mu_f^{\text{budget}})^2}. \tag{3}$$

These family budget values $\Delta\mu_f^{\text{budget}}$ are given as input to the tolerance generation tool and are set by taking into account the stability of the PC currents per family as analysed in Chapter 3. The tolerance on the magnet strength, k_m^{tol}, of a magnet $m \in M_f$ (M_f is the set of magnets in family f) is derived as follows:

1. The *phase response*, $r_{m,s}$, for each $m \in M_f$ is simulated with MADX, by varying its strength, k, by a fixed value ($\Delta k_m = 10^{-5}\,\text{m}^{-2}$) and observing the change in phase advance, $\Delta\mu_s$, within each segment $s \in S$ (S is the set of segments to consider, see Fig. 3) individually:

$$r_{m,s} = \frac{\Delta\mu_s}{\Delta k_m}. \tag{4}$$

2. The phase errors introduced by magnets inside one family can as well be assumed to be independent when their currents are changed individually by functions defined in a given beam process only. This is the case for the main, matching, warm and triplet quadrupoles. The resulting response for the whole family f is defined as the square root of quadratic sum of its member's absolute phase responses:

$$R_{f,s}(\text{Main, Matching, Warm, Triplet}) = \sqrt{\sum_{m\in M_f}|r_{m,s}|^2}. \tag{5}$$

   In case of the trim quadrupoles, the most likely error scenario is a misuse of the tune trim knob, which drives the currents in all trim quadrupoles at the same time. Therefore, for this family the phase errors of individual quadrupoles are correlated and the family response is calculated via the a linear sum:

$$R_{f,s}(\text{Trim}) = \sum_{m\in M_f}|r_{m,s}|. \tag{6}$$

3. From this and $\Delta\mu_f^{\text{budget}}$ the strength tolerance per family and segment is obtained:

$$k_{f,s}^{\text{tol}} = \frac{\Delta\mu_f^{\text{budget}}}{R_{f,s}}. \tag{7}$$

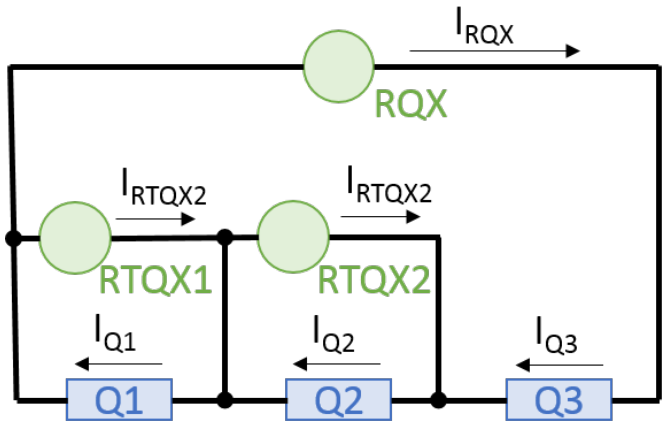

Figure 4: Powering logic of the triplets. The blue rectangles indicate the three triplet quadrupoles (Q1, Q2, Q3) and the three power-converters (RQX, RTQX1, RTQX2) are displayed as the green circles.

4. The final family tolerance, k_f^{tol}, which will be applied to each magnet in f, is defined by the segment in which the minimum tolerance (maximum phase responds) was observed:

$$k_f^{\text{tol}} = \min\left(k_{f,s}^{\text{tol}}\right) \qquad \text{with} \qquad s \in S. \tag{8}$$

The generated strength tolerances k_f^{tol} have to be converted into current tolerances, I^{tol}, within LSA as explained previously.

Special Case: Triplets

Special attention has to be given within the LSA makerules when treating triplet circuits. These circuits consist of three magnets and three power-converters, using a nested powering scheme as sketched in Fig. 4. All other quadrupoles have a one-to-one relation to their power-converter. The currents through the three triplet quadrupoles (Q1, Q2, Q3) are given by:

$$\begin{aligned} I_{Q1} &= I_{RQX} + I_{RTQX1}, & \text{(9a)} \\ I_{Q2} &= I_{RQX} + I_{RTQX2}, & \text{(9b)} \\ I_{Q3} &= I_{RQX}. & \text{(9c)} \end{aligned}$$

The standard makerule for the driving current would simply invert these equations and distribute the current to the power-converters as follows:

$$\begin{aligned} I_{RQX} &= I_{Q3}, & \text{(10a)} \\ I_{RTQX1} &= I_{Q1} - I_{Q3}, & \text{(10b)} \\ I_{RTQX2} &= I_{Q2} - I_{Q3}. & \text{(10c)} \end{aligned}$$

This strategy would not work for the tolerance generation, because e.g. the tolerance for I_{RTQX1} would become zero in case the calculated tolerances for I_{Q1} and I_{Q3} would be equal. Therefore,

the following strategy was chosen to calculate the triplet current tolerances:

$$I^{\mathrm{tol}}_{RQX} = \min\left(\frac{I^{\mathrm{tol}}_{Q1}}{2}, \frac{I^{\mathrm{tol}}_{Q2}}{2}, I^{\mathrm{tol}}_{Q3}\right), \tag{11a}$$

$$I^{\mathrm{tol}}_{RTQX1} = \frac{I^{\mathrm{tol}}_{Q1}}{2}, \tag{11b}$$

$$I^{\mathrm{tol}}_{RTQX2} = \frac{I^{\mathrm{tol}}_{Q2}}{2}. \tag{11c}$$

3 Quadrupole Current Distribution in Physics

The previous chapter focused on the machine protection point of view. However, it also has to be taken into account that if tolerances would be set too tight, the machine availability could be compromised. In this case, the risk of false dumps, due to e.g. fluctuations of the magnet currents, would be increased. To avoid such situation, this chapter describes a detailed analysis on the data of quadrupole currents for the years 2015 to 2017, where the physics operation periods (so-called *Stable Beams*) of all fills with equivalent optics configuration are taken into account. The quadrupoles responsible for online adjustments of the tune, the so-called Tune Trim Quadrupoles, frequently change their current during all periods of the LHC cycle to keep the tune at its reference value. Those are treated separately from the other circuits, which follow pre-programmed current functions.

3.1 Main, Matching, Warm and Triplet Quadrupoles

Normally, the current of the main and warm quadrupoles is only changed during the energy ramp, while the current of the triplets and matching quadrupoles also changes during the β^*-squeeze.[2] As was already mentioned, the currents of these magnet families are set by pre-programmed functions, describing the settings during the different periods of the LHC cycle. For a given machine configuration, those magnets therefore always carry the same current at a certain moment in the cycle. Especially during physics operation the machine settings, and thus the magnet currents, are constant.

For the following analysis, the measured currents, I_{meas}, of all power-converters in these families were extracted from the Logging Database (LDB) in 1 min intervals, repeating the previous data point if no data was available for the given period. Only data during Stable Beams was taken into account. The analysis of this data confirms that the absolute current value of those magnets is always the same within the measurement accuracy of

$$\Delta I_{\mathrm{Main,Matching,Warm}} = \pm 0.03\,\mathrm{A} \tag{12}$$

for the main, matching and warm quadrupoles and

$$\Delta I_{\mathrm{Triplet}} = \pm 0.12\,\mathrm{A} \tag{13}$$

[2]Operating at $\beta^* = 40\,\mathrm{cm}$ with the nominal optics in 2016 some of the main quadrupole circuits around IP1 and IP5 however had to be changed during the squeeze to support the matching quadupoles in order to reach the target β^*. With the ATS optics used since 2017, this adjustment of the main quadrupoles during the squeeze was not necessary anymore.

for the triplets. For most of the triplet magnets an accuracy similar to the other families is found, however one power-converter in IP5 (RQTX2.L5) shows a higher fluctuation rate[3], which therefore defines a higher tolerance for all triplet magnets.

In order to avoid undesired dumps due to current fluctuation, we decided to include a margin of a factor 3 on the tolerance band for those magnet families. The lower tolerance limit imposed by current stability is therefore (rounded):

$$I^{\mathrm{tol}}_{\mathrm{meas}}(\mathrm{Main, Matching, Warm}) \geq 0.1\,\mathrm{A} \tag{14}$$

$$I^{\mathrm{tol}}_{\mathrm{meas}}(\mathrm{Triplet}) \geq 0.4\,\mathrm{A}. \tag{15}$$

3.2 Tune Trim Quadrupoles

The trim quadrupoles (power-converter names are RQTF (focusing) and RQTD (defocusing)) are responsible for setting the tune during the cycle. Whenever the tune needs correction, the strength of those quadrupoles is changed. Their absolute current at a certain stage of the cycle depends on the corrections made before and might thus be different from one fill to the next.

Figure 5 shows a snapshot of the RQTF and RQTD circuit currents at the moment when Stable Beams were declared as a function of the fill number over the years 2015–2017. The operational reference current, I_{ref}, of each PC was used as normalization value. This reference current is the calculated current the PC should operate on. It is set during the commissioning of the given optics in the beginning of each run and it is used as the reference for the PcInterlock. The eight LHC sectors are shown in colour code, but due to their similarity they lie on top of each other.

A clear variation of the current is visible from fill to fill, where the current differences between the measured and the reference value reach up to $\Delta I \approx \pm 3\,\mathrm{A}$, which corresponds to a tune change of about $\Delta Q \approx 0.002$. This number only includes fill to fill variations of the start current in physics. Normally, the tune feedback is switched off during this period, however, occasionally tune corrections are performed, leading to a current variations in the RQTs, which have to be taken into account to define the lower tolerance limit. The histograms displayed in Fig. 6 summarise the current distributions of all RQT circuits over the Stable Beams periods in 2015 (top, left), 2016 (top, right) and 2017 (bottom). Data points of each circuit (RQTFs and RQTDs) were taken every minute during physics operation, normalised to the corresponding reference current and filled in the histograms. In this way, the widths of the distributions provide an estimate of the total current spread observed in physics, including the current variations between fills and over time in one fill.

The bulk of the 2015 distribution is slightly smaller than for 2016. Nevertheless, in 2015 more larger trims up to $\Delta I \approx \pm 3\,\mathrm{A}$ were made, while in 2016 all data points are within a boundary of $\Delta I < \pm 2\,\mathrm{A}$. In 2017 the variation between the families is bigger, as can also be seen from Fig. 5, such that trims up to $\Delta I < \pm 4\,\mathrm{A}$ occurred. The most extreme outliers of these distributions define the absolute lower limit for the tolerance band width:

$$I^{\mathrm{tol}}_{\mathrm{min}} = \pm 4\,\mathrm{A}. \tag{16}$$

This width covers the variations of the initial currents, thus the trim history through the cycle, and the tune corrections in collisions. Nonetheless, a tolerance of this width is considered very

[3]Data from 2016 and 2017 has been analysed. In both years the fluctuation rate for this PC was increased.

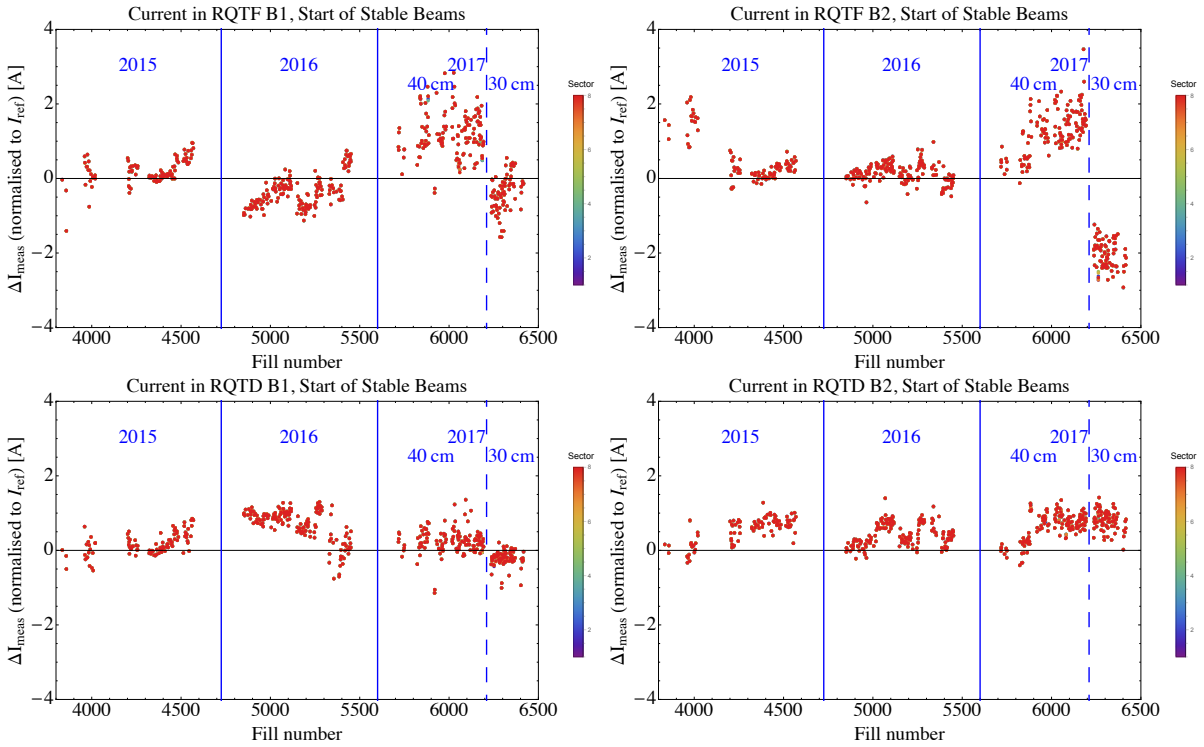

Figure 5: Fill to fill differences in the current of the RQTF (top) and RQTD (bottom) circuits at the start of Stable Beams. Left: Beam 1, right: Beam 2, the different sectors are shown in color code, but due to their similarity for each family they lie on top of each other.

tight and could cause undesired dumps when, e.g., tune corrections on top of a large initial current offset are necessary. The current variations of the RQTs are dominated by desired changes (and not by statistical measurement fluctuations), which are observed to be of similar amount over three years of operation. Therefore, it should be sufficient to include a margin of a factor 2 with respect to Eq. 16. This limits the RQT tolerance band to

$$I_{\text{meas}}^{\text{tol}} \geq 8\,\text{A}. \tag{17}$$

This corresponds to $\Delta Q \approx 0.0056$ in tune units with respect to the reference function.

4 Operational Experience with the new Optics Interlock

4.1 Operational Settings in 2016

With the beginning of the 2016 proton operation the minimum β^* was reduced to 40 cm in IP1 and IP5. In order to provide sufficient protection for the TCTs around these experiments, the last optics point at $\beta^* = 40\,\text{cm}$ was rematched to have more phase margin [16]. The phase advance difference between the MKD and the TCTs in IP1 and IP5 could be optimised to be around 4°. With this adjustment the maximum phase shift allowed was [9]

$$\Delta\mu^{\text{budget}} = 26°. \tag{18}$$

To obtain the PcInterlock settings for the quadrupoles, this amount was distributed over the magnet families as noted in Table 2. The corresponding strength and current tolerances and the

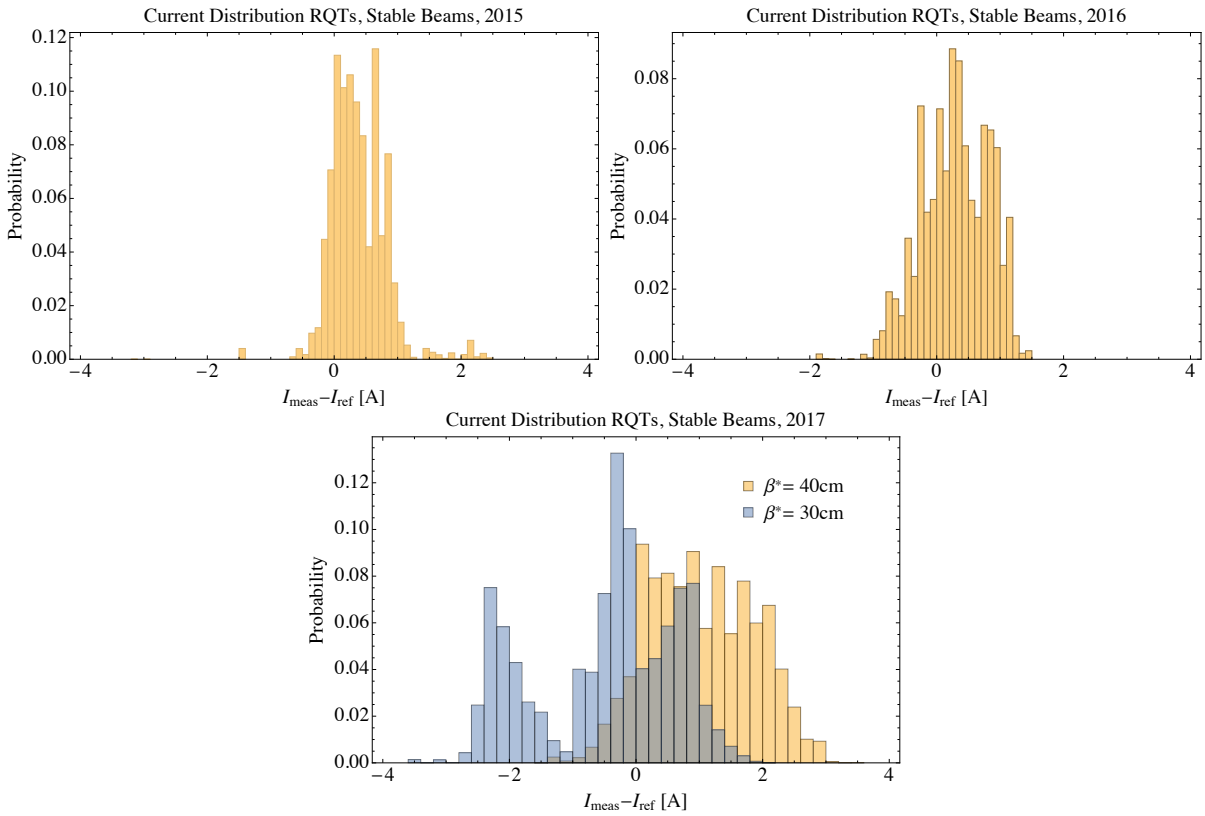

Figure 6: Accumulated current distribution of all trim quadrupole circuits with respect to their reference current. Top, Left: in 2015, right: in 2016, bottom: in 2017 (for $\beta^* = 40\,\text{cm}$ (yellow) and 30 cm (blue)). The three peeks in the 30 cm data from 2017 occur because of the different current offsets in the circuits (see Fig. 5).

lower tolerance limits defined by the observed current fluctuations during physics operation, as discussed in Chapter 3, are listed. According to Eq. 3 only $\Delta\mu^{\text{budget}} = 6.3°$ out of the allowed 26° were used. Nevertheless, from Table 2 it becomes clear that the tolerance settings for all families were still relaxed in 2016 compared to the required minimum defined by the current fluctuations and tune trims.

From a machine protection point of view, the phase interlock is not yet necessary for $\beta^* = 40\,\text{cm}$ [9]. Thanks to that the interlock was not connected to the dump system during the first month of its operation, but registering interlock triggers to gain experience of its functionality and tolerance settings.

4.2 Operational Settings in 2017 (ATS Optics)

For the LHC restart in 2017, the LHC was commissioned with the new Achromatic Telescopic Squeeze (ATS) optics configuration [14]. With the nominal optics configuration, the flexibility in the experimental insertions around IP1 and IP5 is poor at low β^*. Some quadrupoles are being pushed to very low or very high gradients in the matching section and dispersion suppressor. Moreover, the correct-ability of the chromatic aberrations becomes more and more difficult because of the strength limit in the arc sextupoles. The ATS optics configuration enables the operation with smaller β^* by using the matching quadrupoles of the neighbouring straight sections

Quadrupole Families	$\Delta\mu_f^{\text{budget}}$ [°]	k_f^{tol}	I^{tol} **[A]**	$I^{\text{tol}}_{\text{meas}}$ [A]
Main Quadrupoles	1.6	7.7×10^{-6}	4.4	0.1
Main Trim Quadrupoles	5.0	2.5×10^{-4}	22.2	8.0
Triplets	3.3	3.3×10^{-6}	2.2-3.8	0.4
Matching Quadrupoles	1.0	8.7×10^{-6}	0.8-5.2	0.1
Warm Quadrupoles	0.7	1.4×10^{-5}	5.4-7.8	0.1

Table 2: PcInterlock tolerances, k_f^{tol} and I^{tol}, on quadrupole strength and currents operationally used in 2016 with $\beta^* = 40\,\text{cm}$ and $\Delta\mu^{\text{budget}} = 6.3°$. The limits obtained from current fluctuation measurement, $I^{\text{tol}}_{\text{meas}}$, and the applied phase margin per family, $\Delta\mu_f^{\text{budget}}$, are given. Note that even though all magnets of one family have by definition the same tolerances on their strength k, they do not all have the same k-to-I transfer functions. Therefore, I^{tol} can be different for magnets of the same family, which is the case for the triplets, matching and warm quadrupoles. The I^{tol} values of those magnet families are given as ranges between the minimum and maximum used current.

to support the ones in the minimum-β IPs. This generates β-beating waves in the sectors adjacent to the low-β insertions. Assuming a phase advance of exactly $\pi/2$ per arc cell and a proper phasing with respect to the IP, the β-functions will peak at every other sextupole, drastically increasing their chromatic correction efficiency.

Physics operation started at $\beta^* = 40\,\text{cm}$, similarly to 2016, but with a new optics configuration, preparing for the ATS, but not yet using the support of the matching quadupoles from the neighbouring interaction regions. In September the β^* was decreased to $\beta^* = 30\,\text{cm}$, introducing the ATS feature [14]. The phase advances between the MKD and the TCTs are negatively affected by this optics change. With the ATS optics the initial phase difference is already about 26°, implying that the phase is only allowed to drift by $\Delta\mu^{\text{budget}} = 4°$ before the protection of the TCTs and triplets is compromised (see Section 2.3.2).

Table 3 and 4 show the tolerance settings used in 2017 for the two optics configurations. The tolerances were tighter than in 2016, but still comfortably relaxed with respect to the fluctuation minimum in order to gain experience with the active interlock.

Knowing that the current of all families, except the trim quadrupoles, will never be changed by any knob, beam process or operator in physics operation, their limits are set to be around $I^{\text{tol}} = 0.5\,\text{A}$ still leaving some margin with respect to the observed fluctuation limits. If their currents change for any reason the beams need to be dumped for protection. The trim quadrupoles are assigned the largest fraction of the available total phase budget, because they have the largest uncertainty on their currents. The total phase budget of these settings calculates to $\Delta\mu^{\text{budget}} = 5.2°$, which slightly exceeds the value given in Eq. (2). This was allowed because a phase advance measurement revealed a phase shift in the good direction with which the safe phase budget was considered to be $\Delta\mu^{\text{budget}}_{\text{meas}} = 7°$, as described in Section 2.3.2.

Quadrupole Families	$\Delta\mu_f^{\text{budget}}$ [°]	k_f^{tol}	I^{tol} **[A]**	$I^{\text{tol}}_{\text{meas}}$ [A]
Main Quadrupoles	0.2	1.0×10^{-6}	0.6	0.1
Main Trim Quadrupoles	5.0	2.4×10^{-4}	21.8	8.0
Triplets	1.5	1.6×10^{-6}	1.1-1.9	0.4
Matching Quadrupoles	0.5	6.3×10^{-6}	0.5-3.6	0.1
Warm Quadrupoles	0.08	1.5×10^{-6}	0.6-1.4	0.1

Table 3: PcInterlock tolerances, k_f^{tol} and I^{tol}, on quadrupole strength and currents operationally used in 2017 with $\beta^* = 40\,\text{cm}$ and $\Delta\mu^{\text{budget}} = 5.2°$ (see Eq. (3)).

Quadrupole Families	$\Delta\mu_f^{\text{budget}}$ [°]	k_f^{tol}	I^{tol} **[A]**	$I^{\text{tol}}_{\text{meas}}$ [A]
Main Quadrupoles	0.2	0.9×10^{-6}	0.5	0.1
Main Trim Quadrupoles (2017)	5.0	2.2×10^{-4}	20.0	8.0
Main Trim Quadrupoles (2018)	3.0	1.3×10^{-4}	12.0	8.0
Triplets	1.5	1.2×10^{-6}	0.8-1.4	0.4
Matching Quadrupoles	0.5	5.6×10^{-6}	0.5-3.2	0.1
Warm Quadrupoles	0.08	1.5×10^{-6}	0.6-1.4	0.1

Table 4: PcInterlock tolerances, k_f^{tol} and I^{tol}, on quadrupole strength and currents operationally used in 2017/18 with $\beta^* = 30\,\text{cm}$. The only difference between the years is the reduced phase budget of the trim quadrupoles, giving $\Delta\mu^{\text{budget}} = 5.2°$ in 2017 and $\Delta\mu^{\text{budget}} = 3.4°$ in 2018.

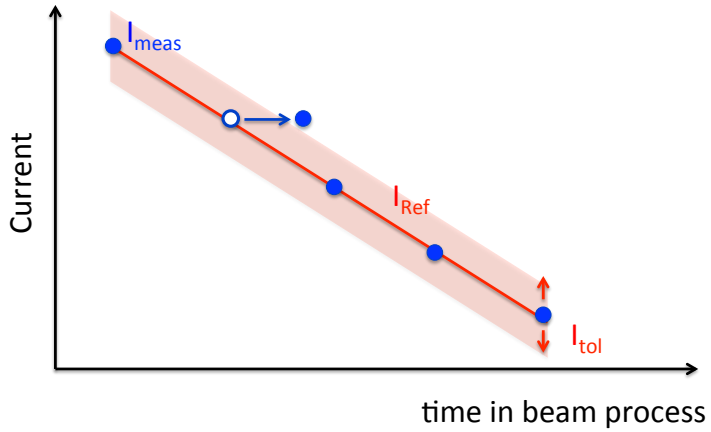

Figure 7: Tolerance evolution during current ramp.

4.3 Operational Settings in 2018 (ATS Optics and β^*-levelling)

So far the optics interlock worked reliably and did not cause any suspicious beam dumps. With this experience the settings for 2018 could be optimised and the tolerances for the trim quadrupoles were further tightened (see Table 4). The nominal $\beta^* = 30\,\text{cm}$ optics configuration is the same as in 2017.

With the restart in 2018 β^*-levelling has been commissioned and operationally used for the first time. For this levelling method, β^* is reduced subsequently when the luminosity has decayed. In the 2018 set-up two β^*-levelling steps from 30 cm via 27 cm to 25 cm are implemented.

Since the procedure is the same as during the Squeeze, the precautions described in Section 4.4 have to be apply for tight tolerance settings. Just after starting a levelling step, the tolerances of the matching quadrupole family have to be opened to account for timing delays between the measured and programmed currents. Right before all quadrupoles reach their final (low β^*) current value, the tolerances need to be closed again. With the currently still rather relaxed tolerances the margins are big enough to cover this issue. If tighter settings are used in the future, this procedure should be programmed into the beam process to be automatically applied for each levelling step.

The tolerance settings used at $\beta^* < 30\,\text{cm}$ apply the same phase budgets as given in Table 4, however the calculated tolerances are about 10–20% tighter at $\beta^* = 25\,\text{cm}$.

4.4 Tolerance Settings during the Squeeze

The current in the quadrupoles naturally changes during the energy ramp and the squeeze. The currents, and so the tolerances, increase during the energy ramp to compensate for the increasing beam rigidity at constant strength (apart from necessary tune corrections). During the squeeze the energy is constant and therefore the tolerances are programmed to be constant as well. For very tight tolerance settings and fast ramp rates, it could happen that the measured current exceeds the tolerances caused by a timing delay with respect to the reference function, as sketched in Fig. 7. In this situation the PcInterlock would trigger and cause an unjustified protection dump. This scenario is avoided by keeping wide, constant tolerance bands during the squeeze and only

close them at the end just before the final optics configuration is reached.

5 Conclusion and Outlook

The PcInterlock was successfully extended to provide interlocks on all LHC quadrupoles. The implementation is completed and the software is running since spring 2016. To test its functionality and to avoid undesired dumps due to wrongly calculated settings or software bugs, the Software Interlock System (SIS) channel was masked (deactivated) until 9 August 2016 such that triggered interlocks are registered but not sent to the beam dump system. Since this date, the software is operationally active and connected to the beam dump system. In 2016 the tolerance settings were very relaxed and no interlocks occurred during Physics. Only during Machine Development (MD) sessions several interlocks were correctly triggered.

With the ATS optics in 2017, the tolerance settings have been tightened to comply with the decreased phase margin in this machine configuration. A total phase budget of $\Delta\mu^{\text{budget}} = 5.3^\circ$ was used in 2017 and reduced to $\Delta\mu^{\text{budget}} = 3.4^\circ$ in 2018, still providing comfortably wide tolerance settings within the limits of the observed current variations. To date no undesired beam dumps were triggered by the optics interlock.

If in the future tighter tolerances would be required, the general $I^{\text{tol}} = 0.5\,\text{A}$ could be further closed to exploit the current fluctuation limit. The triplets are assigned a larger phase budget as the other families with a pre-programmed current cycle, because their effect on the phase advance is large due to the high β-function at their positions. The used values are still a factor 2 above their fluctuation limit and could thus be optimized.

Acknowledgements

We thank R. Bruce, D. Nisbet and D. Wollmann for discussions. We are grateful to M.-A. Galilee, G.-H. Hemelsoet, D. Jacquet, J. Makai and the TE-MPE-SW team for their work and support during the software development.

Acronyms

Acronym	Description
ATS	Achromatic Telescopic Squeeze
IP	Interaction Point
LHC	Large Hadron Collider
LSA	LHC software architecture
MKD	Dump kicker
PC	Power-converter
TCP	Primary collimator
TCS	Secondary collimator
TCT	Tertiary collimator
TCDQ	Collimator between dump kicker and next quadrupole
RQD, RQF	Main focusing (F) and defocusing (D) quadrupoles
RQTD, RQTF	Main Trim Quadrupoles
RQX, RTQX1, RTQX2	Triplet quadrupoles

References

[1] 6th Evian Workshop, 15-17 December 2015, https://indico.cern.ch/event/434129/.

[2] LHC Performance Workshop (Charmonix 2016), 25-28 January 2016, https://indico.cern.ch/event/448109/.

[3] R. Bruce et al., *LHC machine configuration in the 2016 proton run*, LHC Performance Workshop (Chamonix 2016), 25-28 January 2016, https://indico.cern.ch/event/448109/.

[4] *LHC design Report, Vol. 1, The main ring*, CERN-2004-003, June 2004.

[5] R.W. Assmann, *Collimators and beam absorbers for cleaning and machine protection*, Proceedings of the LHC Project Workshop Chamonix XIV, Chamonix, France, 2005, p. 261.

[6] R.W. Assmann, et al., *The final collimation system for the LHC*, Proceedings of the European Particle Accelerator Conference 2006, Edinburgh, Scotland, 2006, p. 986.

[7] R. Bruce, et al., *Simulations and measurements of beam loss patterns at the CERN large hadron collider*, Phys. Rev. ST Accel. Beams 17 (2014) 081004.

[8] R. Bruce, R.W. Assmann, and S. Redaelli *Calculations of safe collimator settings and β^* at the CERN Large Hadron Collider*, Phys. Rev. ST Accel. Beams 18, 061001 (2015)

[9] R. Bruce et al., *Reaching record-low β^* at the CERN Large Hadron Collider using a novel scheme of collimator stetting and optics*, Nucl. Instrum. Meth. A **848** (2017) 19. doi:10.1016/j.nima.2016.12.039

[10] K. Fuchsberger et al. *LHC Orbit Correction Reproducibility and Related Machine Protection*, Proceedings of the International Particle Accelerator Conference 2012 (IPAC'12), New Orleans, LA, USA (2012).

[11] K. Fuchsberger et al., *JMAD - Integration of MADX into the Java World*, Proceedings of the International Particle Accelerator Conference 2010 (IPAC'10), Kyoto, Japan (2010).

[12] https://github.com/jmad

[13] www.cern.ch/madx

[14] S. Fartoukh, *Achromatic telescopic squeezing scheme and application to the LHC and its luminosity upgrade*, Phys. Rev. ST Accel. Beams 16, 111002, Published 19 November 2013.

[15] K. Fuchsberger, A. Calia, M.A. Galile, G.H. Hemelsoet, M. Hostettler, D. Jacquet, J. Makai, M. Schaumann, *Phase Advance Interlocking Throughout the Whole LHC Cycle*, Proceedings of the International Particle Accelerator Conference 2017, Copenhagen, Denmark, 2017, p. 1901 (TUPIK087).

[16] R. de Maria et al., *Squeeze to* 40 cm *with phase constraints*, LHC Beam Operation Committee meeting (LBOC), 8 Mar. 2016, https://indico.cern.ch/event/504322/.

[17] M. Schaumann et al., *PC Interlock status, next steps and feasibility of optics interlocking*, LHC Machine Protection Panel Meeting (MPP), 19 Feb. 2016, https://indico.cern.ch/event/495744/.

[18] M.-A. Galilee et al., *Optics Interlocking within PcInterlock*, TE-MPE-TM Group Meeting, 30 Jun. 2016, https://indico.cern.ch/event/544818/.

[19] A. Calia et al., *PC Interlock: Recent updates and status*, LHC Machine Protection Panel Meeting (MPP), 26 Aug. 2016, http://indico.cern.ch/event/564015/.

[20] M. Schaumann et al., *PC Interlock - experience from 2016 operation*, Joint meeting of Collimation Working Group and LHC Machine Protection Panel, 6 Feb. 2017, https://indico.cern.ch/event/610454/.

[21] LHC Performance Workshop (Chamonix 2017), 23-27 January 2017, https://indico.cern.ch/event/580313/.